Int. J. Electrochem. Sci., 7 **(2012)** 8035 - 8051

International Journal of
ELECTROCHEMICAL
SCIENCE
www.electrochemsci.org

Voltammetric and Impedance studies of Phenols and Its Derivatives at Carbon Nanotubes/Prussian Blue Films Platinum Modified Electrode

Abolanle S. Adekunle[1,2,*], *Omotayo A. Arotiba*[1], *Bolade O. Agboola*[3,*], *Nobanathi W. Maxakato*[1], *Bhekie B. Mamba*[1]

[1] Department of Applied Chemistry, University of Johannesburg, P.O. Box 17011, Doornfontein, 2028, South Africa
[2] Department of Chemistry, Obafemi Awolowo University, Ile-Ife, Nigeria
[3] Department of Petroleum Chemistry and Engineering, American University of Nigeria, Yola, Nigeria
[*]E-mail: sadek2k@yahoo.com, aadekunle@oauife.edu.ng; bolade.agboola@aun.edu.ng, bolade_agboola@yahoo.co.uk

Received: 5 July 2012 / *Accepted:* 18 August 2012 / *Published:* 1 September 2012

The electrochemical oxidation of phenol (Ph), 4-chlorophenol (4-ClPh) and 4-nitrophenol (4-NPh) at a platinum electrode modified with and without multi-walled carbon nanotubes/Prussian blue nanocomposite in a pH 7.0 phosphate buffer electrolyte was investigated by cyclic voltammetry (CV) and impedance measurements. The modified electrodes were characterised using techniques such as transmission electron microscopy (TEM), electron X-ray dispersive spectroscopy (XRD), cyclic voltammetry (CVs) and electrochemical impedance spectroscopy (EIS). The phenol produced an irreversible CV oxidation peak whose potential increased for 4-ClPh and 4-NPh derivatives. Pt-MWCNT-SO_3^--PB electrode gave the highest electro-oxidation current compared to the other electrodes studied. The oxidation of the phenol compounds was not completely diffusion controlled especially at higher scan rate, and the electrode was characterized by some level of adsorption. The degree of adsorption was depicted by the Tafel values of 4292.4, 663.2 and 203.8 $mVdec^{-1}$ for Ph, 4-ClPh and 4-NPh respectively. The limits of detection were in the micro molar range and the Gibbs free energy change (ΔG^o) due to adsorption was estimated as -33.8, -35.8 and -36.0 $kJmol^{-1}$ for Ph, 4-ClPh and 4-NPh. Impedance data showed that the MWCNT-SO_3^--PB film was so porous and behaved as a pseudocapacitor towards the oxidation of the analytes.

Keywords: Phenols; Platinum electrode; Prussian blue nanoparticles; Oxidation; Adsorption; Impedance measurement.

1. INTRODUCTION

Phenols and the chlorinated and alkylated derivatives are classified as priority pollutants due to the health risk associated with their toxicity [1]. Industrial effluents containing phenols as pollutants include effluents or waste from pharmaceuticals, dyes, plastic, food, oil, detergents, pesticide and herbicide, coal, pulp and paper industry, textiles, chemical synthesis, etc. [2,3]. They are extremely dangerous since they are harmful to organisms even at low concentrations [4]. Phenols ingestion (1 g) through oral exposure has been reported to be lethal, with symptoms such as muscle weakness and tremors, loss of coordination, paralysis, convulsions and respiratory arrest [2]. Phenol derivatives belong to a class of chemicals that are easily adsorbed through skin and mucous tissues. Their toxicity affects a wide number of organs: primarily lungs, liver, kidneys, and the genito-urinary system [1,5]. Chlorophenols are derivatives of phenols used in the synthesis of herbicides and pesticides. They are toxic compounds, chemically stable, highly resistant to biological degradation and pose a threat to humans and animals if persistently present in the environment [6, 7]. They can also be found in industrial effluents, mainly from cellulose plants. The OH group of chlorophenols (CPs) confers to them an acidic character and capability to dissolve in water. Due to their constant presence in industrial waste and consequently their carcinogenic risk for humans, methods for the detection of phenol and chlorophenols and quantification are important. Phenol and chlorophenols can be detected by means of spectrophotometric [8], chromatographic [9] and electrochemical methods [10] but the electrochemical method is the most efficient since it takes a shorter time with no chemical derivatization and gives very reproducible results [2]. In fact, electrochemical oxidation of phenol is reported to be the effective and attractive method from the economical point of view of removal of phenolic compounds from waste water [11, 12]. However, electrochemical oxidation of phenols on solid surface is usually associated with adsorbed oxidation intermediates which poison the surface due to polymer formation during the oxidation process. Thus, there is a need for surface modification in order to reduce drastically or completely eradicate the effect. Therefore, there has been increased research by scientists in solving these challenges since they impact on the sensitivity and the limit of detection of phenols and their derivatives by fabricated sensors and other analytical instruments. The electroactive species on the modified electrode surface usually retain their own properties and allow the development of processes such as pre-concentration, electrocatalysis [2]. Bare electrode materials such as gold, platinum, glassy carbon and boron doped diamond electrodes have been tested for phenols and chlorophenols oxidations [6, 13-16]. Similarly, the oxidation of phenols and chlorophenols on modified electrodes with different kinds of catalysts have also been reported [2, 6, 17, 18], while the oxidation of chlorophenols on GC modified with polymeric films of Ni(II)tetrasulphophthalocyanine at pH 11 have also been reported [19].

Prussian blue (PB) is an iron cyanide complex ($Fe_4(III)[Fe(II)(CN)_6]_3$) often used as an electron-transfer mediator on modified electrodes during electrochemical processes. Its application in catalysis has also been reported, for example in the detection hydrogen peroxide [20, 21], Hemoglobin, [22], glucose [23] and oxygen [24]. The use of Pt-composites as electrode materials for phenolic compounds oxidation is a viable alternative due to the excellent activity of this electrocatalyst particularly when the loading of Pt nanoparticles is controlled.

Therefore, the objective of this study was to explore the resistance of the platinum electrode modified with multi-walled carbon nanotubes/Prussian blue nanocomposite (Pt-MWCNT-SO_3^--PB) towards poisoning by polyphenols intermediates during phenol (Ph), 4-chlorophenol (4-ClPh) and 4-nitrophenol (4-NPh) oxidation, particularly because the various methods of limiting platinum fouling have been proposed and promising results concerning phenol oxidation on Pt based composite electrodes have been documented [25-29]. In addition, this study also probed and provided insight in the pertinent information on the complex reaction mechanism associated with Ph, 4-ClPh and 4-NPh adsorption on the Pt-MWCNT-SO_3^--PB electrode using electrochemical impedance studies.

2. EXPERIMENTAL

2.1 Materials and Reagents

Multi-walled carbon nanotubes were purchased from Sigma Aldrich Chemicals and were acid treated to introduce sulphonic functional group (SO_3^-) using a known procedure [29]. $FeCl_3$, $K_3[Fe(CN)_6]$, KCl, Phenol (Ph), 4-chlorophenol (4-ClPh) and 4-nitrophenol (4-NPh) and other chemicals and reagents were of analytical grade and sourced from Sigma-Aldrich chemicals. Ultra pure water of resistivity 18.2 MΩcm was obtained from a Milli-Q Water System (Millipore Corp., Bedford, MA, USA) and was used throughout the experiments. A phosphate buffer solution (0.1 M PBS) of pH 7.3 was prepared with appropriate amount of $NaH_2PO_4.2H_2O$ and $Na_2HPO_4.2H_2O$, and the pH was adjusted with 0.1 M H_3PO_4 or NaOH.

2.2. Equipment and Procedure

The working electrode, bare platinum (d = 1.6 mm) was purchased from BASi, USA. The energy dispersive x-ray spectra (EDX) were obtained from NORAN VANTAGE instrument (USA). Transmission electron microscopy (TEM) characterisation was performed with a Tecnai G2 Spirit FEI company Transmission Electron Microscope, Orgeon (USA). Electrochemical experiments were carried out using an Autolab Potentiostat PGSTAT 302N (Eco Chemie, Utrecht, and The Netherlands) driven by GPES and Frequency Response Analyser software. Electrochemical impedance spectroscopy (EIS) measurements were performed between 10 kHz and 0.1 Hz using a 5 mV rms sinusoidal modulation in 5 mM $[Fe(CN)_6]^{4-}/[Fe(CN)_6]^{3-}$ solution at a fixed dc potential of 0.2 V and in the Ph, 4-ClPh and 4-NPh solutions at their peak potential of oxidation. The reference and counter electrodes used were Ag|AgCl in saturated KCl and platinum wire, respectively. A bench top BOECO pH meter, model BT-600 (Germany), was used for pH measurements. All solutions were de-aerated by bubbling argon for 10 minutes prior to each electrochemical experiment. All experiments were performed at 25 ± 1 °C.

2.3. Electrode modification procedure

A platinum electrode was cleaned by gentle polishing in aqueous slurry of alumina powder, Sigma-Aldrich (grain size <100 nm) on a SiC-emery paper, mirror finished on a Buehler felt pad and was subjected to ultrasonic vibration in absolute ethanol and water successively. Pt-MWCNT-SO_3^- was prepared by a drop-dry method using 10 µL drop of the MWCNT solution (0.1 mg MWCNT in 1 ml DMF). The volume and concentration values of MWCNT solution used were chosen after optimisations using different values and based on their respective voltammetric responses were carried out. The Pt-MWCNT-SO_3^- electrode was dried in an oven at 50 ^oC for about 2 min. Electrodeposition of Prussian blue on the Pt-MWCNT-SO_3^- and its activation was done by adopting a method earlier reported [31]. The modified electrode will be denoted as Pt-MWCNT-SO_3^-PB. Other electrodes investigated are bare Pt and Pt-PB.

3. RESULTS AND DISCUSSION

3.1 Comparative FTIR, XRD, SEM, TEM, and EDX spectra

Figure 1 shows the comparative FTIR spectra of the MWCNT-SO_3^-, PB and MWCNT-SO_3^--PB. In the MWCNT-SO_3^- spectrum, the bands at 1384, 1044 cm^{-1} are respectively attributed to S=O and S-O stretching modes of the sulphonic acid group (-SO_3^-) in MWCNT-SO_3^-. Also, the band at around 1653 cm^{-1} is due to the vibration mode of C=C bonds of the CNT structure. As can be seen in the MWCNT-SO_3^--PB spectrum, upon modification, all these peaks (1384, 1044, 1653 cm^{-1}) drastically reduced in intensities, indicating that the MWCNT-SO_3^- had now been modified with PB. Further evidence of modification of MWCNT-SO_3^- with PB can be seen in the MWCNT-SO_3^--PB spectrum, the sharp band at 2078 cm^{-1} is attributed to PB $C{\equiv}N_{str}$ band found in MWCNT-SO_3^--PB and PB spectra but absent in MWCNT-SO_3^- spectrum.

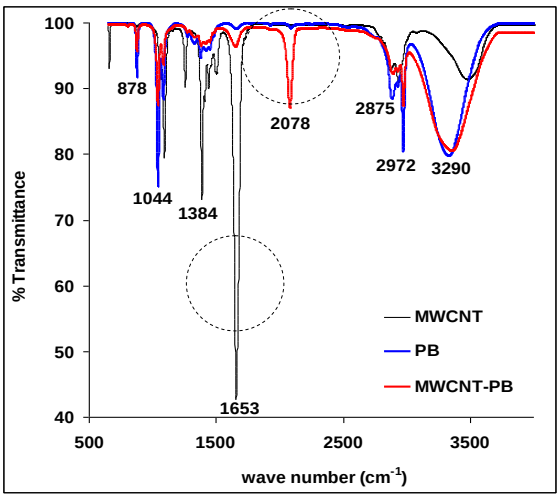

Figure 1. Comparative FTIR spectra of MWCNT-SO_3^-, PB and MWCNT-SO_3^--PB nanoparticles

The corresponding XRD spectra for the MWCNT-SO_3^-, PB and the MWCNT-SO_3^--PB nanoparticles are shown in Figure 2. Unlike the well defined and resolved peaks obtained for the PB and the MWCNT-SO_3^--PB, the MWCNT-SO_3^- was the only one that gave a very broad and an un-resolved peak which is mainly as a result of the amorphous nature of the CNT particles. The resolved peaks of the PB nanoparticles confirm the crystalline nature of the iron complex as depicted by the TEM and the SEM images. The XRD spectrum for MWCNT-SO_3^--PB gave peaks with a higher intensity than PB alone. This behavior is associated with the large surface area created by the MWCNT-SO_3^- supports, which allowed for more deposition of uniformly and evenly distributed PB nanoparticles.

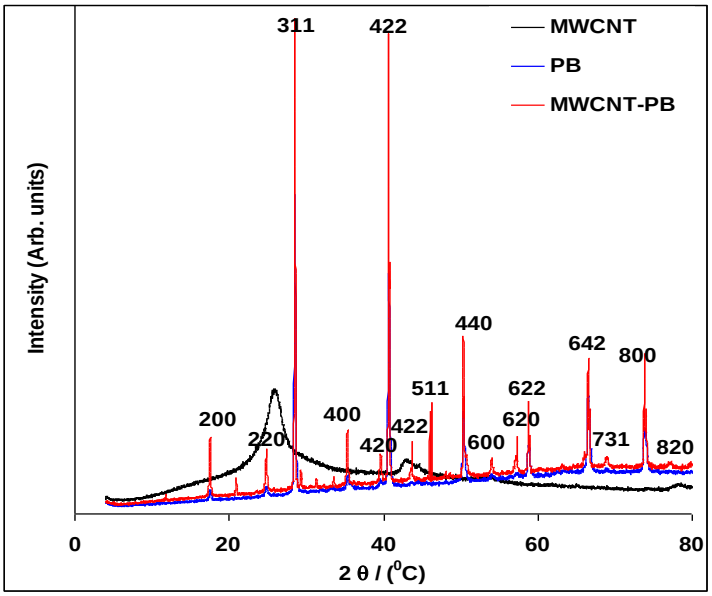

Figure 2. Comparative XRD spectra of MWCNT-SO_3^-, PB and MWCNT-SO_3^--PB nanoparticles

Different characteristic peaks for Fe (at 2θ = 17.9, 25.1, 29.1, 30.4, 35.6, 40.1, 43.9, 46.6, 50.6, 54.6, 57.6, 60.1, 68.9, 70.8, 74.3, and 77.0), corresponding to Miller indices (200), (220), (311), (222), (400), (420), (422), (611), (444), (600), (620), (622), (642), (731), (800) and (820) were observed. The XRD data indicated a cubic crystal system for the resultant PB nanoparticles (Molecular. Formula = $C_{18}Fe_7N_{18}$).

Using Debye-Scherrer formula [32]:

$$d = \frac{K\lambda}{B\cos\theta} \quad (1)$$

where d is the average crystal size; K is a constant (0.89); λ is the wavelength (1.78901 nm) used; B is the full width at half maximum of the peak, θ is the Bragg's angle of the XRD peak, the crystal sizes of the PB particles were estimated from three prominent peaks to be ~ 17.5 nm.

Figures 3 (a) shows the transmission electron microscope (TEM) images of the PB nanoparticles and the images confirm the crystalline nature of the PB nanoparticles, which came together to form an aggregate. After calibrating the scale of the TEM image using the UTHSCSA Image Tool for windows version 3.0, the PB nanoparticle sizes of the 15–35 nm range were obtained which agreed with the particle size obtained from the XRD result. The EDX profile (Fig. 3b) revealed the presence of Fe peaks which represent Fe^{2+} and Fe^{3+} of the PB nanoparticles.

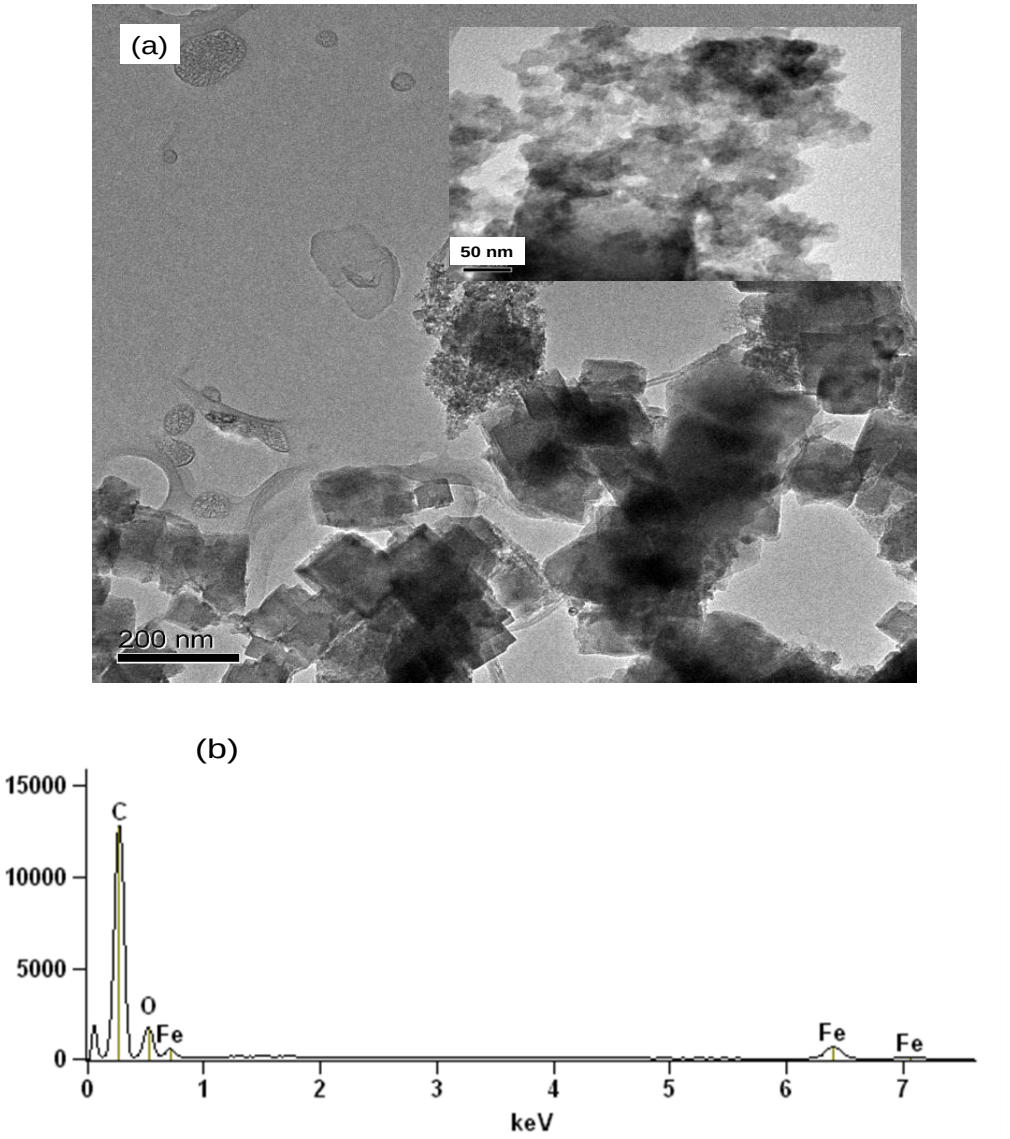

Figure 3. (a) HRSEM image of PB nanoparticles (b) EDX spectrum PB nanoparticles.

3.2. Electrocatalytic oxidation of phenol, 4-chlorophenol and 4-nitrophenol at the electrodes.

Figure 4a compares the current response (1st scan) of the modified electrode in phosphate buffer solution (pH 7.3) containing 10 mM phenol (Ph), 4-chlorophenol (4-ClPh) and 4-nitrophenol (4-NPh) respectively at 25 mVs^{-1}. From Figure 4, the Ph, 4-ClPh and 4-NPh oxidation signal (absent in the PBS electrolyte) was observed for the studied electrodes Pt, Pt-MWCNT-SO_3^-, Pt-PB and Pt-

MWCNT-SO_3^--PB at an anodic peak potentials of *ca* 0.7, 0.65 and 0.9 V respectively. In all the analytes, Pt-MWCNT-SO_3^--PB electrode gave the highest oxidation current of 108.0, 128.0 and 162.0 μA in Ph, 4-ClPh and 4-NPh respectively, which was almost 12 and 9 times greater than 9.23 μA (Ph), 13.7 μA (4-ClPh) and 18.7 μA (4-NPh) recorded for the analytes on bare Pt electrode.

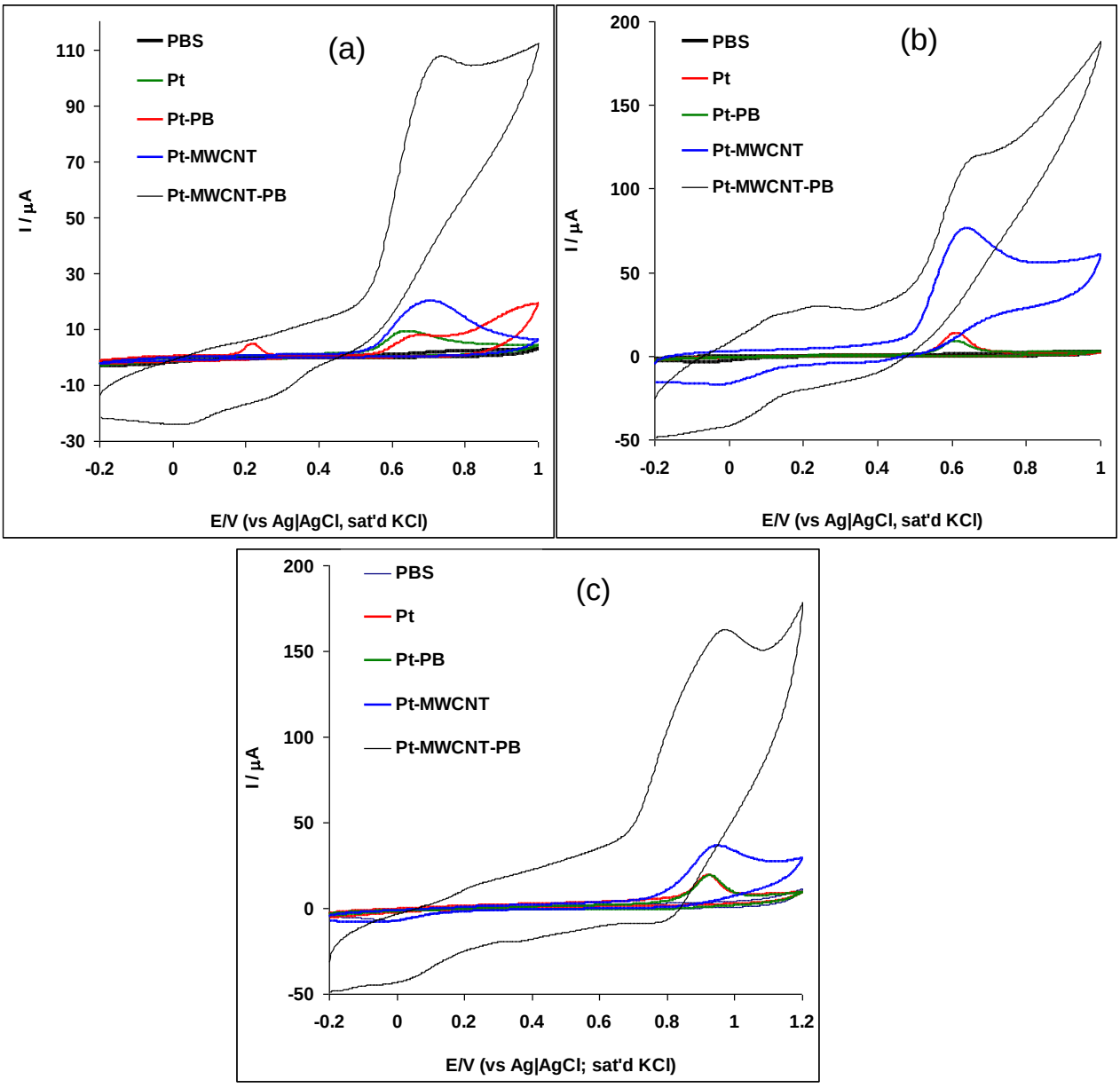

Figure 4. Figure 4 compares the current response (1st scan) of the modified electrode in phosphate buffer solution PBS (pH 7.3) containing (a) 10 mM phenol (Ph), (b) 10 mM 4-chlorophenol (4-ClPh) and (c) 10 mM 4-nitrophenol (4-NPh) respectively, scan rate: 25 mV s^{-1}.

The results obtained were consistent with other literature reports on enhanced phenols oxidation current on modified electrodes [2, 4, 33]. Also, the initial potential of catalysis at Pt-MWCNT-SO_3^--PB electrode is 50, 170 and 180 mV lower for Ph, 4-ClPh and 4-NP compared with the

other electrodes investigated. However, after the second scan, a complete loss in oxidation signals of the analytes (Ph, 4-ClPh and 4-NP) was observed on the bare Pt electrode as exemplified in Fig. 5a for Ph, while a relatively small drop (7-14%) in the analytes oxidation currents was noticed on the Pt-MWCNT-SO_3^--PB electrode (Ph, 4-ClPh and 4-NP respectively shown in Fig. 5b-d). This implies that the bare Pt became deactivated due to surface fouling by the formation of polyphenols derivatives of the analytes. This finding further suggests the capability of Pt-MWCNT-SO_3^--PB modified electrode to withstand electrode fouling that is due to the formation of polymerised Ph, 4-ClPh and 4-NPh oxidation products [18], a phenomenon which has long plagued phenol and its derivatives electrochemical detection and quantification in food, pharmaceuticals and industrial waste.

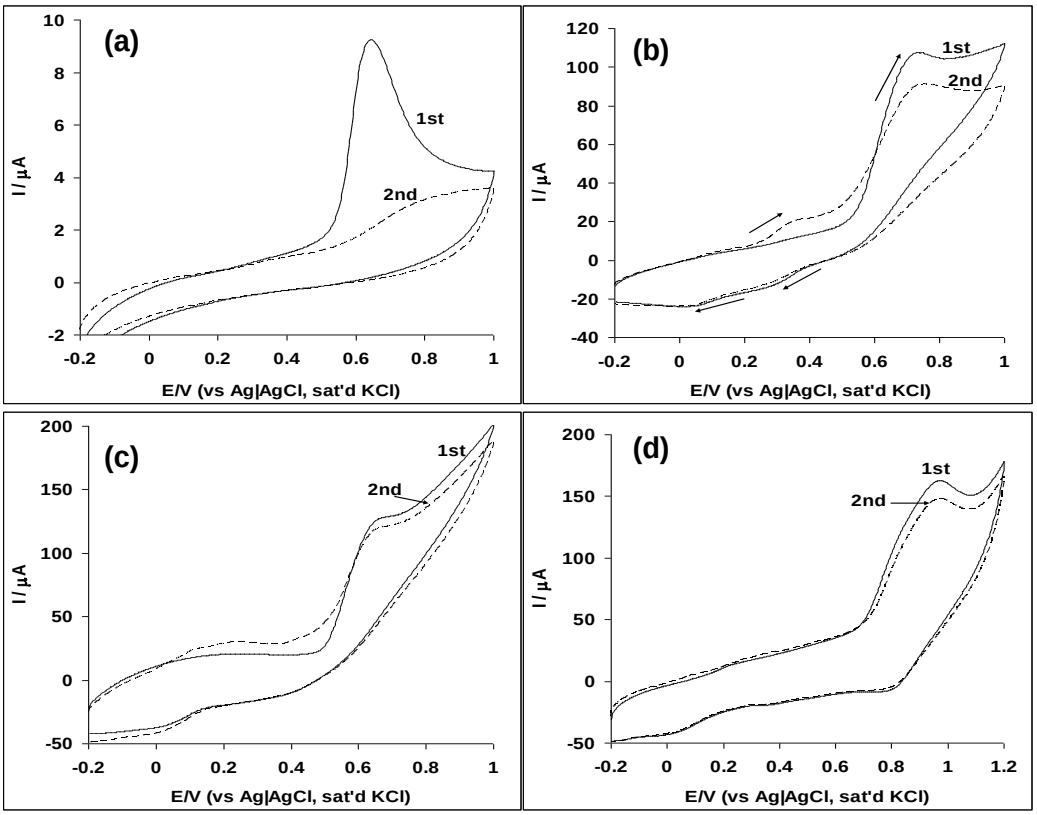

Figure 5. Comparative current response (1st and 2nd scan) showing the effect of passivation on (a) bare Pt electrode in PBS (pH 7.3) containing 10 mM Ph, (b) Pt-MWCNT-SO_3^--PB electrode in PBS (pH 7.3) containing 10 mM Ph, (c) Pt-MWCNT-SO_3^--PB electrode in PBS (pH 7.3) containing 10 mM 4-ClPh and (d) Pt-MWCNT-SO_3^--PB electrode in PBS (pH 7.3) containing 10 mM 4-NPh.

Other reasons for the enhanced performance of the Pt-MWCNT-SO_3^--PB electrode even after several voltammetry cycles could be due to: (i) the presence of the porous nature of MWCNT-SO_3^- and the PB films which allow free passage of the analytes, and (ii) the reduction of formed platinum oxides back to Pt during the reverse process thus reactivating the surface of the electrode for further oxidation of the phenols.

The results obtained in this study revealed that the activity of the Pt-MWCNT-SO_3^--PB electrode was acceptable since it satisfied at least two requirements for a good electro-catalyst which

includes high current peak density for the process investigated; and low energy (*E*/*V*) to supply the current peak density [34]. Similarly, the synergy between MWCNT-SO_3^- and PB on Pt-MWCNT-SO_3^--PB electrode is significant judging from the analytes' improved current response and lower energy compared to the other electrodes. The MWCNT-SO_3^- increased surface area allow for more PB deposition, therefore exposing the phenols to more catalytic sites. Finally, it was observed that electro-oxidation of 4-ClPh and 4-NPh on the Pt-MWCNT-PB electrode was more favoured (in terms of peak current, see Fig 4) compared to that of Ph. This could probably be due to the negative inductive effect (-I) of the highly electronegative chlorine (Cl) and the nitrogen (N) substituents, which contributes to the ease of deprotonation of the OH group on 4-ClPh and 4-NPh during oxidation. In a related study, the low polymerization rate of 2,4,6 TCP (tri-chlorophenol) was related to the probability of its high dechlorination rate [6], since an earlier study concluded, on the basis of gas chromatography–mass spectrometry (GC–MS), that CP polymerization occurs *via* two routes: (i) the quinol–ether route (without chlorine elimination) and (ii) the nucleophilic-radical substitution (SR_N1) route (with an elimination of chlorine from *ortho* and/or *para* positions) [35].

Based on previous reports on phenol oxidation at modified electrodes [1, 6, 27], the reactions in Scheme 1 below were assumed to be taking place at the Pt-MWCNT-SO_3^--PB modified electrode.

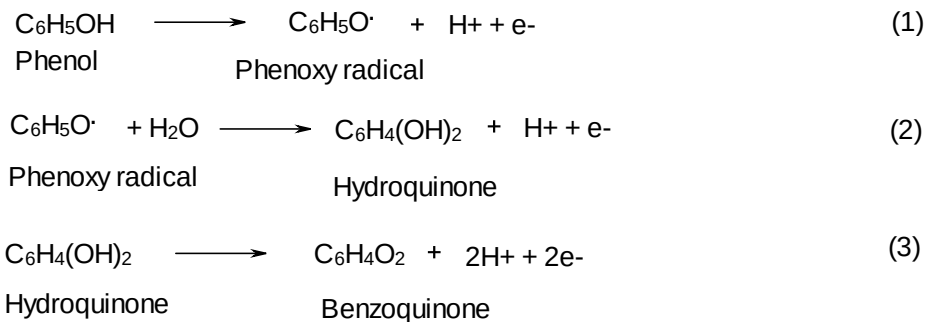

Scheme 1. Electro-oxidation of phenol at Pt-MWCNT-SO_3^--PB modified electrode

Phenol underwent degradation to produce the phenoxy radical through the loss of one electron (Eq 1). Further oxidation of the phenoxy radical to hydroquinone was facilitated by hydroxyl radicals (formed from water) adsorbed on the electrode (Eq 2). The hydroquinone degrades and forms benzoquinone with a loss of two electrons (Eq 3).

Since PT-MWCNT-SO_3^- exhibited good electrochemical properties towards the analytes, further experiments reported in this work were carried out using this electrode.

3.3. Electrochemical Impedance Study

Figure 6a and 6b show the Nyquist and Bode plots for Pt-MWCNT-SO_3^--PB electrode during Ph, 4-ClPh and 4-NPh oxidation at 0.70 V vs Ag|AgCl sat'd KCl. Inset in Figure 6a is the electrical circuit used in the fitting of the electrochemical impedance data for Ph and 4-ClPh, while circuit $R_s(C[R_{ct}C])$ (not shown) was used in the fitting of 4-NPh impedance data. In the circuit model, R_s is

the solution/electrolyte resistance, R_{ct} denotes the charge-transfer resistance, C_{film} describes the high pseudocapacitive nature of the system while CPE relates to the porous nature of the electrode. The lower R_{ct} for the Pt-MWCNT-SO_3^--PB electrode in all the analytes compared well with that of the bare Pt (Table 1) indicating faster electron transport and more favorable oxidation of the analytes on the electrode, enabled by the porous and the high electroactive surface area of the electrode which allowed for easy contact with the analytes.

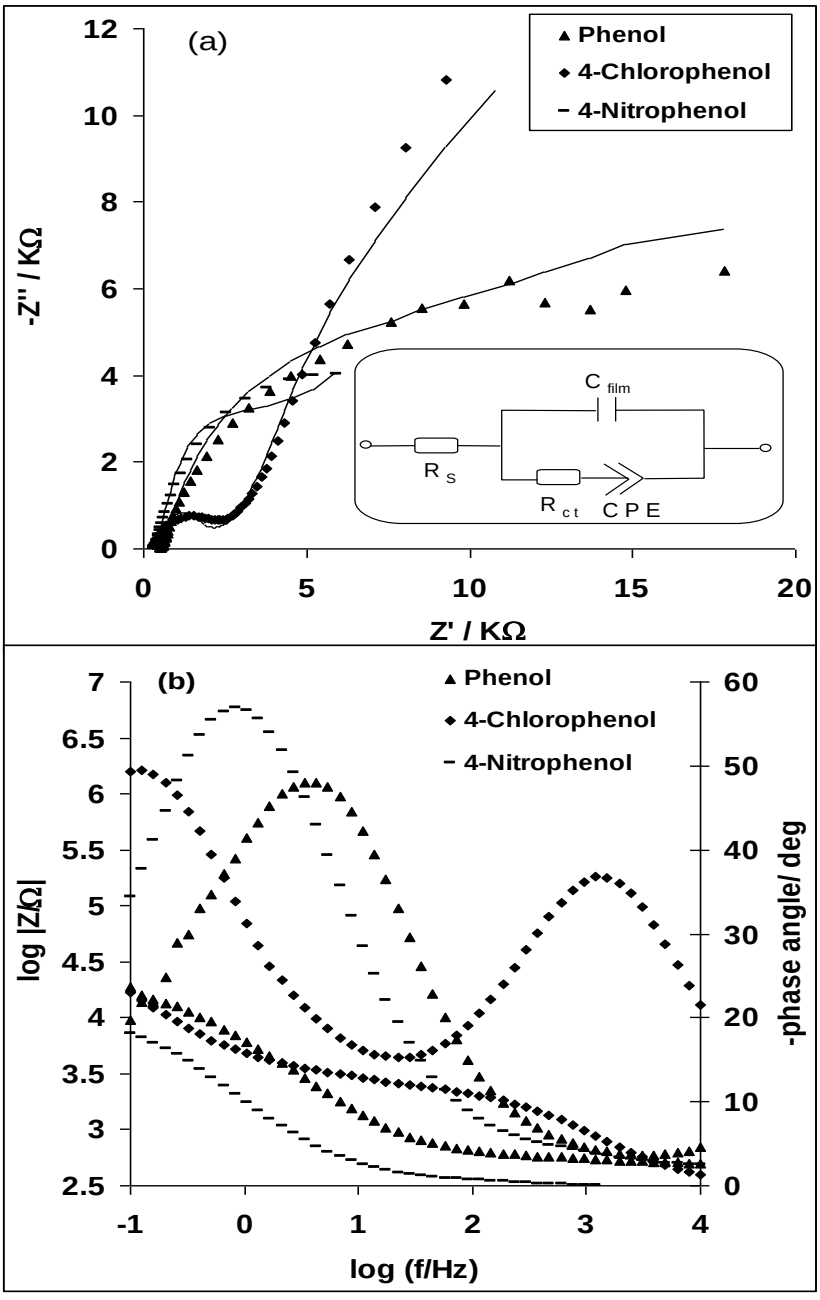

Figure 6. Figure 5 presents (a) Nyquist plots and (b) Bode plots for the Pt-MWCNT-SO_3^--PB electrode during the oxidation of 10 mM of Ph, 4-ClPh and 4-NPh respectively in phosphate buffer solution (pH 7.3). Inset in Figure 5a is the electrical circuit used in the fitting of the impedance data.

Table 1. Impedance data for Pt and Pt-MWCNT-SO_3^--PB electrodes in PBS (pH 7.3) containing 10 mM phenol, 4-chloropheno and 4-nitrophenol, respectively, at 0.70 V vs Ag|AgCl sat'd KCl. Note that the values in parentheses are the percent errors of data fitting.

Electrode	Impedimetric parameters					
	R_s/KΩ	C/nF	R_{ct}/KΩ	Q/μF	n	C/μF
Phenol						
Pt	0.585 (6.416)	20.23 (5.26)	2.016 (6.50)	3.066 (1.210)	0.558 (0.610)	-
Pt-MWCNT-PB	185.6 (38.632)	9780.0 (6.087)	0.578 (18.044)	74.0 (4.180)	0.2802 (9.621)	-
4-chloroPhenol						
Pt	0.573 (13.209)	24.47 (13.33)	1.566 (14.99)	3.685 (2.859)	0.564 (1.387)	-
Pt-MWCNT-PB	0.372 (4.940)	265.7 (12.949)	0.453 (15.611)	124.8 (4.141)	0.4244 (4.507)	-
4-nitroPhenol						
Pt	0.632 (7.115)	1413.0 (9.785)	9.11 (14.087)	-	-	6.74 (9.808)
Pt-MWCNT-PB	0.328 (2.394)	91400.0 (5.893)	2.050 (6.367)	-	-	748.0 (15.419)

Bode plot of –phase angle vs. log (f/Hz) obtained for the different PB layers (Figure 6b) gave phase angles less than -90^o which is expected in ideal capacitive behavior confirming the presence of CPE and pseudo-capacitive behavior of Pt-MWCNT-SO_3^--PB electrodes towards Ph, 4-ClPh and 4-NPh. This behavior has also been related to adsorption of reaction intermediates at the electrode [36,37]. Also, the *n* values obtained (Table 1) were less than 1.0, indicating the pseudo-capacitive nature of the electrodes in the analyte. Presently, there is very limited information on the electrochemical impedance study of Ph, 4-ClPh and 4-NPh oxidation especially at platinum modified electrodes. From one available report on chlorophenols oxidation on glassy carbon electrode at pH 11 buffer electrolyte, C. Berr´ıos et al. (2008) reported that the impedance measurements clearly show that the polyphenolic film fouling the electrode surface is non-porous and non-conducting for 2-CP and 2,4-CP, while in the case of 2,4,6-TCP it is porous and allows the oxidation of 2,4,6-TCP in solution to continue especially at higher potential (0.55 V) probably reflecting the degradation of the polymeric films at higher potential [6]. Therefore, the impedance behavior of their reported system was also as complex as the one observed in this study by the different circuit model used in the fitting of 4-NPh impedance data. The complexity of the spectra can be attributed to several factors such as electrode structure, level of substitution on the phenol, position of substitution and the potential at which the impedance study was carried out.

3.4. Stability study

The Pt-MWCNT-SO_3^--PB electrode was run repetitively (30 cycles) in 10 mM solution of the analytes at 50 mVs^{-1}. Noteworthy, the oxidation signal of the analytes could still be observed even after the tenth scan (Fig. 7). This is an indication that the electrode exhibited higher stability.

Conducting polymers such as PBT (poly(2,2'-bithiophene)), PMT (poly(3-methylthiophene)), and PBSBT (poly[4,4'-bis(butylsulphanyl)-2,2'-bithiophene) coating on Pt electrode led to the loss of the phenol oxidation signal after the second scan and beyond, which suggests that the polymeric electrode coating formed an insulating layer which did not prevent passivation from occurring [1].

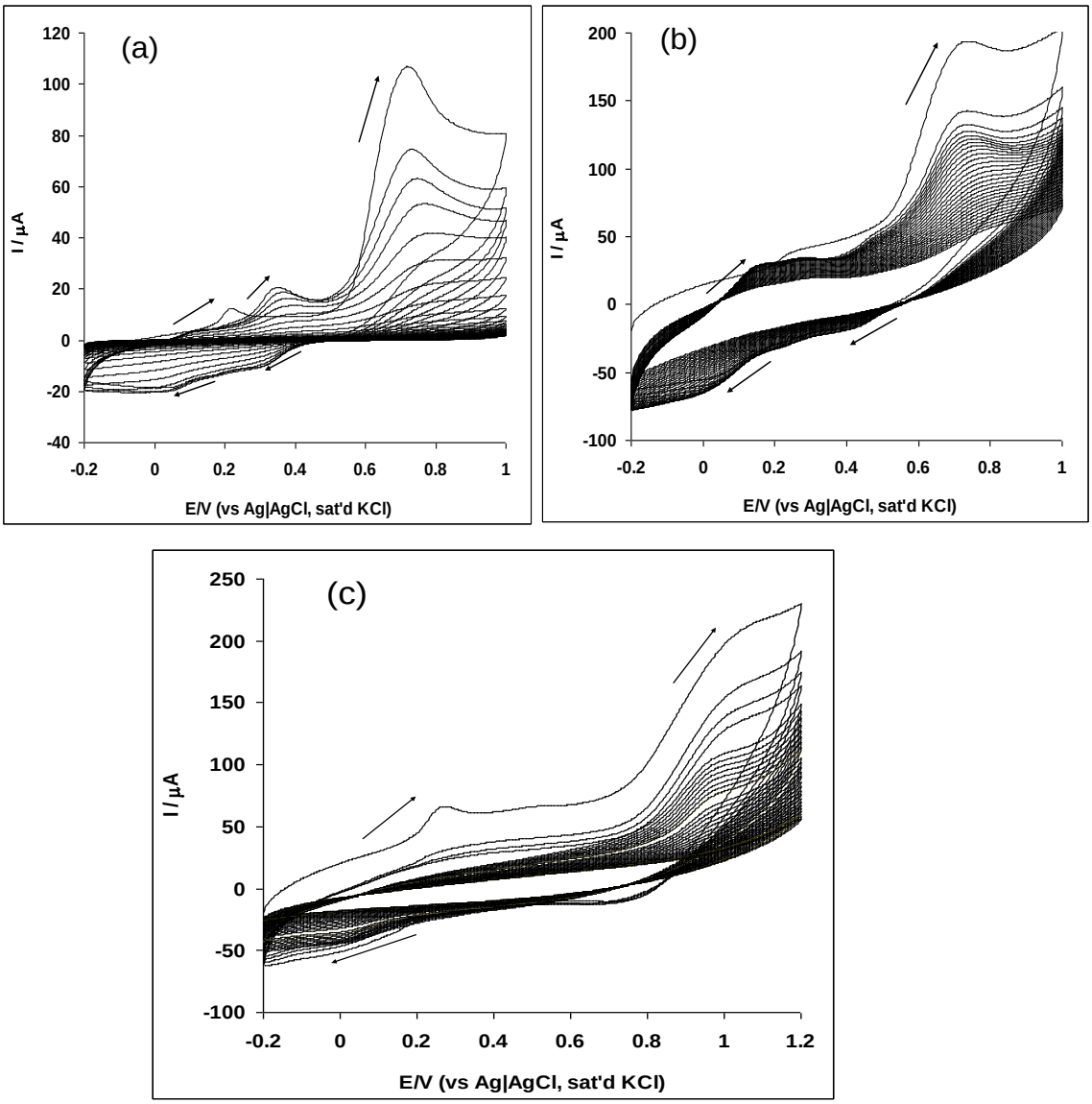

Figure 7. Repetitive cyclic voltammograms (20 cycles) of (a) Pt-MWCNT-SO_3^--PB electrode in PBS (pH 7.3) containing 10 mM Ph, (b) Pt-MWCNT-SO_3^--PB electrode PBS (pH 7.3) containing 10 mM 4-ClPh and (c) Pt-MWCNT-SO_3^--PB electrode in PBS (pH 7.3) containing 10 mM 4-NPh (scan rate: 50 mVs^{-1}).

Also, in this study, the Pt-MWCNT-SO_3^--PB electrode was less poisoned in 4-ClPh and 4-NPh Figs. 7b and 7c) compared to Ph (Fig. 7a) as indicated by the gradual and insignificant drop in the oxidation peak with increasing number of scans. Loss of 4-ClPh and 4-NPh oxidation signals started

occurring after the 20th scan. This behavior can be attributed to the ease of deprotonation of ClPh and 4-NPh which delayed the formation of polyphenols oxidation products.

3.5. Scan rate study

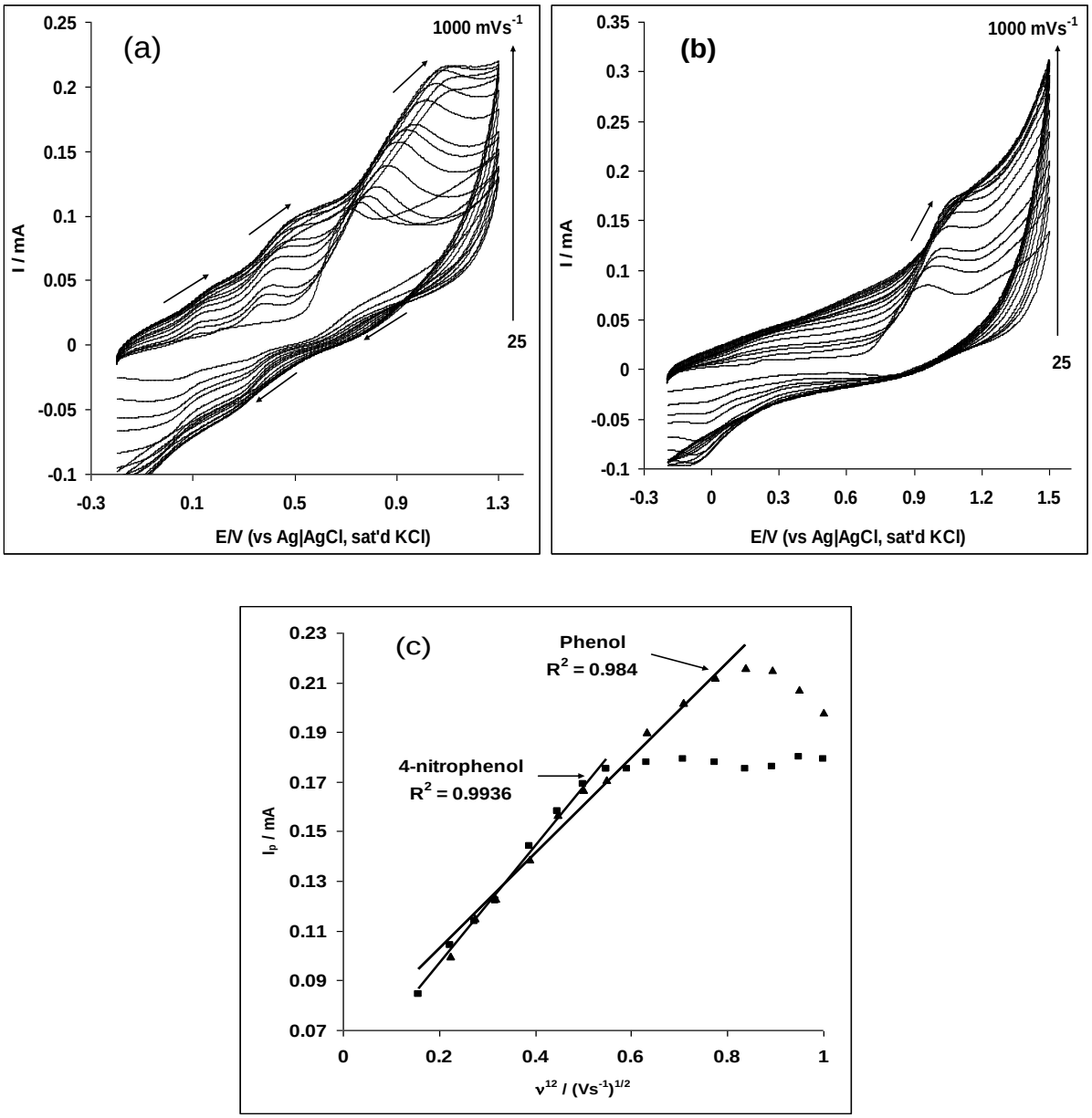

Figure 8. Scan rate study (25-1000 mVs^{-1}) of the Pt-MWCNT-SO_3^--PB electrode in PBS (pH 7.3) containing (a) 10 mM Ph and (b) 10 mM 4-NPh. (c) is the plot of I_p vs. $\nu^{1/2}$ for both Ph and 4-NPh.

The effect of the scan rate (ν) (scan rate: 25-1000 mVs^{-1}) at constant concentration (10 mM) on the electrocatalytic oxidation of Ph, 4-ClPh and 4-NPh was investigated using Pt-MWCNT-SO_3^--PB electrode and represented with Ph and 4-NPh (Figs 8a and b). At 25 mVs^{-1}, the anodic peaks around

0.1 and 0.2 V respectively were attributed to Pt/Pt^{2+} and PB (Fe^{2+}/Fe^{3+}) redox processes, and the anodic peak at 0.7 or 0.65, or 0.9 V corresponded to Ph, 4-ClPh and 4-NPh oxidation signals, and was ascribed to the phenol/quinone process where benzoquinone was identified as the phenol oxidation intermediate [1, 6, 26]. The process was mediated by the Fe^{2+}/Fe^{3+} of the PB nanoparticles. Generally the oxidation peak potentials for the molecules shifted slightly positive with increasing scan rates. Plots of I_p vs. $\nu^{1/2}$ (Fig. 7c) gave a straight line especially at a lower scan rate, but there was deviation at high scan rates indicating that the process of electro oxidation of the analytes on the electrode was not completely diffusion controlled. Similarly the current function plots ($I_p/\nu^{1/2}$ vs. ν) obtained for the analytes gave the characteristic curves attributed to a coupled electrochemical-chemical (EC_{cat}) reaction processes at the electrode. From the Tafel equation for a totally irreversible diffusion-controlled process [42], plots of E_p versus logν gave a linear relationship and a slope ($b/2 = \partial E_p/\partial(\log\nu)$) of 2.1462, 0.3316 and 0.1019 $Vdec^{-1}$, corresponding to Tafel values (b) of 4292.4, 663.2 and 203.8 $mVdec^{-1}$ for Ph, 4-ClPh and 4-NPh respectively, and are higher than the theoretical value of 118 $mVdec^{-1}$ for a one-electron process in the rate-determining step, suggesting adsorption or the involvement of reaction intermediates on the electrode surface [37, 38]. The highest Tafel value (4292.4 $mVdec^{-1}$) for Ph further confirmed the high level of adsorption and electrode poisoning experienced after several scans in the analyte compared to the others. The lowest Tafel value (203.8 $mVdec^{-1}$) for 4-NPh supports the higher oxidation current reported for the analyte due to the minimum electrode adsorption effect.

3.6. Electroanalysis of Phenol, 4-chlorophenol and 4-nitrophenol

Two sensitive electrochemical methods, adsorptive stripping voltammetry (LSV) and chronoamperometry (CA) were used to investigate the impact of varying concentrations of the analytes to current response at the Pt-MWCNT-SO_3^--PB platform. However, using CA, no reasonable current response was obtained with increasing concentration due to poisoning effect hence; LSV is a more conceivable technique since it gave reasonable analytical data.

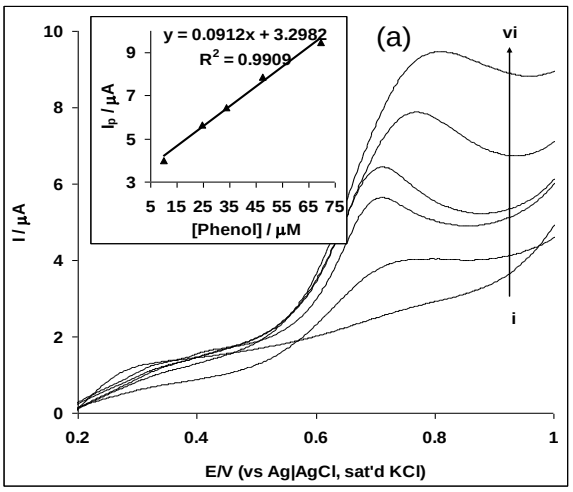

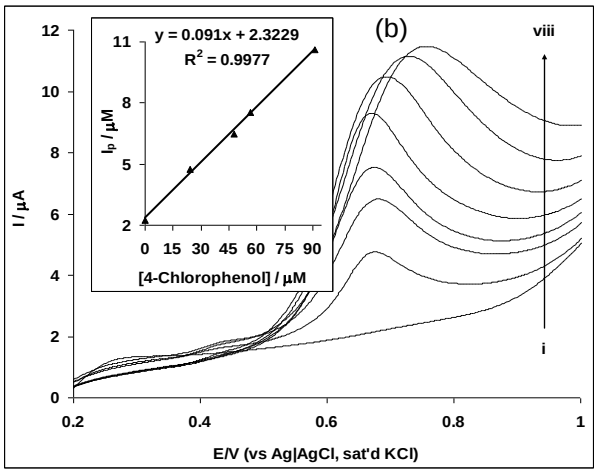

Figure 9. Typical linear sweep response of Pt-MWCNT-SO_3^--PB electrode in (a) PBS (pH 7.3) containing different concentrations of Ph (0.0, 9.9, 24.4, 33.8, 47.6, and 69.8 µM (i - vi)), (b) PBS (pH 7.3) containing different concentrations of 4-ClPh (0.0, 24.4, 47.6, 56.6, 69.8, 90.9, 111.1 and 130.0 µM (i - viii)). Inset in (a) and (b) are the linear plots obtained from peak current response I_p vs. Ph and 4-ClPh concentration respectively.

Moreover, the adsorptive behavior of the polyphenols molecules or its intermediates on the electrode is a limitation to ultra-low detection of the analyte using the chronoamperometric methodology. Figure 9 shows examples of linear sweep voltammograms obtained in Ph and 4-ClPh. The current was recorded after stirring the electrode in solution for at least 5 minutes.

From the plots of I_p versus concentration (Insets in Fig. 9), the values of the limit of detection (LoD = 3.3 δ/m, where δ is the relative standard deviation of the intercept of the y-coordinates from the line of best fit, and *m* the slope of the same line) were 7.04, 4.71 and 11.76 □M for Ph, 4-ClPh and 4-NPh respectively. The LoD value obtained for phenol (7.04 µM) in this study is a lot less compared to 500 µM reported for the analyte on poly(3,4-ethylenedioxythiophene)-poly(styrene sulphonate) composite (PEDOT/NaPSS) platinum electrode using similar technique (LSV), but less than 10 µM reported for the analyte on the same electrode using square wave voltammetry (SQWV) technique [1].

The adsorptive properties of the analytes was further established by estimating their electrochemical adsorption equilibrium constant *(β)* using the Langmuir Adsorption Isotherm theory [24]. From Langmuir adsorption isotherm theory (Eqn.8), the plot of the ratio of analyte concentration and the catalytic current ([Analyte]/I_{cat}) versus analyte concentration [Analyte] (not shown) gave a straight line from which it can be concluded that this was an adsorption controlled electrochemical process.

$$\frac{[\text{Phenol}]}{I_{cat}} = \frac{I}{\beta I_{max}} + \frac{[\text{Phenol}]}{I_{max}} \qquad (8)$$

The adsorption equilibrium constant for the Pt-MWCNT-SO_3^--PB electrode in the analytes was estimated to be β (0.83± 0.05), (1.86 ± 0.05) and (2.06 ± 0.02) x 10^3 M^{-1} for Ph, 4-ClPh and 4-NPh

oxidation. Thus, using Eqn. 9, the Gibbs free energy change due to adsorption was estimated as -33.8, -35.8 and -36.0 kJmol^{-1}.

$$\Delta G^o = - RTln\ \beta. \quad (9)$$

Since there was no significant difference in their standard free energy of adsorption (ΔG^o), the adsorption of the analytes on Pt-MWCNT-SO_3^--PB electrode followed the same kinetics which involve the formation of benzoquinone intermediates as supported by previous reports on the mechanism of phenol electro-oxidation at modified electrodes [1,6,27].

4. CONCLUSION

The electrochemical oxidation of phenol (Ph), 4-clorophenol (4ClPh) and 4-nitrophenol (4-NPh) on Pt electrode modified with or without MWCNT-SO_3^--PB nanocomposite was carried out using cyclic voltammetry and electrochemical techniques. Better results were obtained in terms of the onset potential of catalysis, peak current and slower passivation of the electroactive surface using Pt-MWCNT-SO_3^--PB electrode. Using cyclic voltammetry, the Pt-MWCNT-SO_3^--PB electrode displayed higher stability and more enhanced anti-fouling effects over other electrodes, and more importantly, in comparison with other Pt based electrodes, the Pt-MWCNT-SO_3^--PB electrode exhibited more resistance to electrode poisoning by oxidisation intermediates. The electrochemical impedance studies showed that the electrode was very porous and exhibited pseudo-capacitance behaviour towards electron transfer due to the adsorbed analyte oxidation intermediate. Also, adsorptive properties of the analytes was further established by estimating their electrochemical adsorption equilibrium constant *(β)* using the Langmuir Adsorption Isotherm theory. The Ph, 4-ClPh and 4-NPh were detected at micro molar concentration levels using linear seep voltammetry. The LoD of 7.04 μM obtained for phenol is relatively low in comparison with other Pt based electrodes. The electrode has the potential to be used as an efficient electrochemical sensor for Ph, 4-ClPh and 4-NPh detection but it is important to note that using this kind of electrode configuration as a platform for phenolic sensing requires adequate knowledge of the adsorption phenomenon in order to choose an appropriate electrochemical technique for reliable analytical data.

ACKNOWLEDGEMENTS
This project was financially supported by the University of Johannesburg and the DST/Mintek Nanotechnology Innovation Centre (NIC). ASA thanks the University of Johannesburg for post-doctoral fellowship and Obafemi Awolowo University Nigeria for the research sabbatical leave.

References

1. M. A. Heras, S. Lupu, L. Pigani, C. Pirvu, R. Seeber, F. Terzi, C. Zanardi, *Electrochim Acta,* 50 (2005)1685.
2. L. Fern´andez, C. Borr´as, H. Carrero, *Electrochim Acta* 52 (2006) 872.

3. X. Yang, R. Zou, F. Huo, D. Cai, D. Xiao, *J. Hazard. Mater.*, 164 (2009) 367.
4. Z. Mojović, N. Jović-Jovičić, P. Banković, M. Žunić, A. Abu Rabi-Stanković, A. Milutinović-Nikolić, D. Jovanović, *Applied Clay Science*, 53 (2011) 331.
5. C. Nistor, J. Emn´eus, L. Gorton, A. Ciucu, *Anal. Chim. Acta*, 387 (1999) 309.
6. C. Berr´ıos, R. Arce, M.C. Rezende, M.S. Ureta-Za˜nartu, C. Guti´errez, *Electrochim. Acta*, 53 (2008) 2768.
7. Toxic Substance Control Act, Environmental Protection Agency,Washington, DC, USA, 1979.
8. W. Frenzel, S. Krekler, *Anal. Chim. Acta*, 310 (1995) 437.
9. F.E.O. Suliman, S.S. Al-Kindi, S.M.Z. Al-Kindy, H.A.J. Al-Lawati, *J. Chromatogr.* A, 1101 (2006) 179.
10. J.M. Skowron´ ski, P. Krawczyk, *Chemical Engineering Journal*, 152(2009) 464.
11. G. Chen, *Sep. Purif. Technol*., 38 (2004) 11.
12. C.A. Martinez-Huitle, S. Ferro, *Chem. Soc. Rev.*, 35 (2006) 1324.
13. M.S. Ureta-Zanartu, P. Bustos, C. Berrios, M.C. Diez, M.L. Mora, C. Gutierrez, *Electrochim. Acta*, 47 (2002) 2399.
14. G.W. Muna, N. Tasheva, G.M. Swain, *Environ. Sci. Technol.*, 38 (2004) 3674.
15. M.A. Rodrigo, P.A. Michaud, I. Duo, M. Panizza, G. Cerisola, C. Comnellis, *J. Electrochem. Soc.*, 148 (2001) D60.
16. M.S. Ureta-Zanartu, P. Bustos, M.C. Diez, M.L. Mora, C. Gutierrez, *Electrochim. Acta*, 46 (2001) 2545.
17. K. Peeters, K. D. Wael, D. Bogaert, A. Adriaens, *Sens. Actuat. B*, 128 (2008) 494.
18. B. Agboola, T. Nyokong, *Electrochim. Acta*, 52 (2007) 5039.
19. M.S. Ureta-Zanartu, C. Berr´ıos, J. Pavez, J. Zagal, C. Guti´errez, J.F. Marco, *J. Electroanal. Chem.*, 553 (2003) 147.
20. S. Han, Y. Chen, R. Pang, P. Wan, *Ind. Eng. Chem. Res.*, 46 (2007) 6847.
21. Y. Shan, G. Yang, J. Gong, X. Zhang, L. Zhu, L. Qu, *Electrochim. Acta*, 53 (2008) 7751.
22. Y. Xian, Y. Zhoua, Y. Xian, L. Zhouc, H. Wang , L. Jin, *Anal. Chimic. Acta*, 546 (2005) 139.
23. Y. Miao, J. Chen, X. Wu, J. Miao, *Coll. Surf. A: Physicochem Eng Aspects*, 295 (2007)135.
24. A-M Gurban, T. Noguer, C. Bala, L. Rotariu, *Sens. Actuat. B*, 128 (2008) 536.
25. C.H. Tzang, C.W. Li, J. Zhao, M. Yang, *Anal. Lett.*, 38 (2005) 1735.
26. S. Lupu, C. Lete, M. Marin, N. Totir, P.C. Balaure, *Electrochim. Acta*, 57 (2009) 1932.
27. T. Spataru, M. Marcu, A. Banu, E. Roman, N. Spataru, *Electrochim. Acta*, 54 (2009)3316.
28. Z. Mojovic, A. Milutinovic-Nikolic, S. Mentus, D. Jovanovic, *Chem. Eng. Technol.*, 32 (2009) 738.
29. T. Spataru, Nicolae Sp˘ataru, *J. Hazard. Mater.*, 180 (2010) 777.
30. Z-P. Sun, X-G. Zhang, Y-Y. Liang, H-L. Li, *J. Power Sources*, 191 (2009) 366.
31. X. Che, R. Yuan, Y. Chai, J. Li, Z Song, W. Li, X. Zhong, *Coll. Surf. B: Biointerfaces*, 84 (2011) 454.
32. Y-K. Sun, M. Ma, Y. Zhang, N. Gu, *Coll. Surf. A: Physicochem Eng Aspects*, 245 (2004) 15.
33. M.A.M. Cartaxo, K. Ablad, J. Douch, Y. Berghoute, M. Hamdani, M.H. Mendonça, J.M.F. Nogueira, M.I.S. Pereira, *Chemosphere*, 86 (2012) 341.
34. R. G. Freitas, M. C. Santos, R. T. S. Oliveira, L. O. S. Bulhoes, E. C. Pereira, *J. Power Sources*, 158(2006) 164.
35. Z. Ezerskis, Z. Jusys, *J. Appl. Electrochem.*, 32 (2002) 543.
36. J. Bisquert, H. Randriamahazaka, G.Garcia-Belmonte, *Electrochim. Acta*, 51 (2005) 627.
37. A.S. Adekunle, J. Pillay, K.I. Ozoemena, *Electrochim. Acta*, 55 (2010) 4319.
38. J.N. Soderberg, A.C. Co, A.H.C. Sirk, V.I. Birss, *J. Phys. Chem. B*, 110 (2006) 10401.
39. H.X. Ju, L. Donal, *J. Electroanal. Chem.*, 48 (2000) 150.